



Alejo, A. and Green, A. and Ahmed, H. and Robinson, A.P.L. and Cerchez, M. and Clarke, R. and Doria, D. and Dorkings, S. and Fernandez, J. and McKenna, P. and Mirfayzi, S.R. and Naughton, K. and Neely, D. and Norreys, P. and Peth, C. and Powell, H. and Ruiz, J.A. and Swain, J. and Willi, O. and Borghesi, M. and Kar, S. (2016) Numerical study of neutron beam divergence in a beam-fusion scenario employing laser driven ions. Nuclear Instruments and Methods in Physics Research Section A: Accelerators, Spectrometers, Detectors and Associated Equipment, 829. pp. 176-180. ISSN 0168-9002 , <http://dx.doi.org/10.1016/j.nima.2016.05.057>

This version is available at <https://strathprints.strath.ac.uk/56869/>

Strathprints is designed to allow users to access the research output of the University of Strathclyde. Unless otherwise explicitly stated on the manuscript, Copyright © and Moral Rights for the papers on this site are retained by the individual authors and/or other copyright owners. Please check the manuscript for details of any other licences that may have been applied. You may not engage in further distribution of the material for any profitmaking activities or any commercial gain. You may freely distribute both the url (<https://strathprints.strath.ac.uk/>) and the content of this paper for research or private study, educational, or not-for-profit purposes without prior permission or charge.

Any correspondence concerning this service should be sent to the Strathprints administrator: strathprints@strath.ac.uk

The Strathprints institutional repository (<https://strathprints.strath.ac.uk>) is a digital archive of University of Strathclyde research outputs. It has been developed to disseminate open access research outputs, expose data about those outputs, and enable the management and persistent access to Strathclyde's intellectual output.

Numerical study of neutron beam divergence in a beam-fusion scenario employing laser driven ions

A. Alejo^a, A. Green^a, H. Ahmed^a, A.P.L. Robinson^b, M. Cerchez^c, R. Clarke^b, D. Doria^a, S. Dorkings^b, J. Fernandez^b, P. McKenna^d, S.R. Mirfayzi^a, K. Naughton^a, D. Neely^b, P. Norreys^{b,1}, C. Peth^c, H. Powell^d, J.A. Ruiz^e, J. Swain^f, O. Willi^c, M. Borghesi^a, S. Kar^{a,*}

^aCentre for Plasma Physics, School of Mathematics and Physics, Queen's University Belfast, BT7 1NN, UK

^bCentral Laser Facility, Rutherford Appleton Laboratory, Didcot, Oxfordshire, OX11 0QX, UK

^cInstitut für Laser-und Plasmaphysik, Heinrich-Heine-Universität, Düsseldorf, 40225, Germany

^dDepartment of Physics, SUPA, University of Strathclyde, Glasgow, G4 0NG, UK

^eColegio Los Naranjos, Fuenlabrada, Madrid, 28941, Spain

^fRudolf Peierls Centre for Theoretical Physics, University of Oxford, Oxford, OX1 3NP, UK

Abstract

The most established route to create a laser-based neutron source is by employing laser accelerated, low atomic number ions in fusion reactions. In addition to benefiting from the high reaction cross-sections at moderate energies of the projectile ions, the anisotropy in the neutron emission is another important feature of beam-fusion reactions. Using a simple numerical model based on neutron generation in a pitcher-catcher scenario, anisotropy in the neutron emission was studied for the deuterium-deuterium fusion reaction. Simulation results are consistent with the narrow-divergence ($\sim 70^\circ$ full width at half maximum) neutron beam recently obtained from an experiment employing multi-MeV deuteron beams of narrow divergence (upto 30° FWHM depending on the ion energy) accelerated by a sub-petawatt laser pulse from thin deuterated plastic foils via the Target Normal Sheath Acceleration mechanism. By varying the input ion beam parameters, simulations show that a further improvement in the neutron beam directionality (i.e. reduction in the beam divergence) can be obtained by increasing the projectile ion beam temperature and cut-off energy, as expected from the interactions with higher power lasers at upcoming facilities.

Keywords: laser, neutron, beam fusion

1. Introduction

Fast neutron sources driven by high-power lasers have gained substantial interest over the last decades for a range of potential applications in medicine [1], security [2, 3], material science [4] and high energy density physics research [5]. Furthermore, deploying compact moderators closely coupled to laser-driven fast neutrons sources would allow the development of intense sources of thermal and epithermal neutrons, which would extend the range of applicability of laser-based sources. With the rapid progress in laser technology, aiming towards developing higher repetition rate lasers of higher powers, laser-driven neutron sources can, in principle, complement the research activities currently pursued at

conventional accelerator-driven spallation sources. Although these large scale facilities produce substantially higher fast neutron fluxes, a key interest for laser-driven neutron sources lies in the neutron burst duration, which is substantially shorter than that produced at spallation facilities.

With the current laser systems, neutron yields up to of the order of 10^{10} neutrons/shot have been shown experimentally ([6, 7] and references therein), by employing laser driven ions to generate neutrons from secondary catcher targets via beam-fusion reactions. In addition to the advantage of the ultra-short pulse duration, directionality/anisotropy in the neutron emission is another important characteristic resulting from the beam-fusion reactions. The total neutron yield from a fusion reaction scales with the product of fusing ion densities and cross-section σ , which, for the most common reactions, reaches high values for centre-of-

*Corresponding author.

Email address: s.kar@qub.ac.uk

33 mass energy in the MeV-10s of MeV range [8]. In a
 34 pitcher-catcher scenario, where neutrons are produced
 35 by bombarding the laser-driven ions on a suitable con-
 36 verter target, anisotropy arises from the nuclear reac-
 37 tion kinematics, which strongly depends on the atomic
 38 mass of the fusing nuclei and velocity of the projectile
 39 ions [6]. In addition, the strong angular dependence
 40 of the differential cross-section for light nuclei reac-
 41 tions helps producing neutron fluxes strongly peaked
 42 along the incident ion-beam direction, even while us-
 43 ing moderate energy (10s of MeV) ions as acceler-
 44 ated at currently available laser intensities [9]. In this
 45 context, fusion reactions based on low atomic mass
 46 nuclei, such as ${}^7\text{Li}(p,n){}^7\text{Be}$, ${}^9\text{Be}(p,n){}^9\text{B}$, ${}^{13}\text{C}(p,n){}^{13}\text{N}$,
 47 $d(d,n){}^3\text{He}$, $T(d,n){}^4\text{He}$, ${}^7\text{Li}(d,xn)$, ${}^7\text{Be}(d,xn)$, are partic-
 48 ularly relevant, which would not only allow obtaining
 49 higher neutron yield, but higher peak flux by producing
 50 a narrow cone beam of neutrons. A highly beamed neu-
 51 tron flux would be extremely helpful towards improving
 52 transport capabilities as well as efficient moderation of
 53 the neutrons to thermal and epithermal energies by us-
 54 ing compact, closely-coupled, directional moderators.

55 Anisotropic emission of the neutron beam is start-
 56 ing to be realized in experiments. In addition to
 57 the anisotropy intrinsic to the beam-fusion, as dis-
 58 cussed above, the neutron beam divergence from a typ-
 59 ical laser-driven pitcher-catcher source also depends
 60 strongly on the divergence of the projectile ions - the fi-
 61 nal neutron beam divergence from the catcher will be a
 62 convolution of the divergence of the input ion beam and
 63 the neutron beam divergence expected for a collimated
 64 beam of ions.

65 In this paper we show a simple model for simu-
 66 lating the neutron production from light nuclei reac-
 67 tions in a pitcher-catcher scenario, and to study the
 68 effect of ion beam parameters (divergence and spec-
 69 trum) on the neutron generation. The neutron beam
 70 divergence estimated by our model from $d(d,n){}^3\text{He}$ reac-
 71 tion in a beam-fusion scenario, while using laser-
 72 driven deuterium beam produced via the Target Normal
 73 Sheath Acceleration (TNSA) mechanism[9], compares
 74 well with the data obtained from a recent experiment
 75 [6]. A systematic study show that the neutron beam di-
 76 vergence can be reduced significantly (to a few tens of
 77 degrees) by increasing the input ion beam temperature,
 78 which, according to the current understanding of the
 79 TNSA mechanism, is achievable using the intense lasers
 80 that will be available at the upcoming facilities[10, 11].

81 2. Simulation design and method

82 Alternative to the usual Monte-Carlo approach [12,
 83 13] to simulate neutron generation in a beam-fusion sce-
 84 nario, the model described in this paper (as discussed
 85 below) takes advantage of the tabulated angularly-
 86 resolved neutron yield, that can be found in the liter-
 87 ature, obtained for a mono-energetic, pencil beam of
 88 ions impinging onto a catcher at normal incidence. The
 89 main interaction that is taken into account in our simple
 90 model is the effect of a multi-energy, divergent beam
 91 of ions, as typically produced by the TNSA mecha-
 92 nism, towards the angular distribution of emitted neu-
 93 trons from a secondary catcher target. The schematic of
 94 the setup used in our model is shown in Fig. 1.

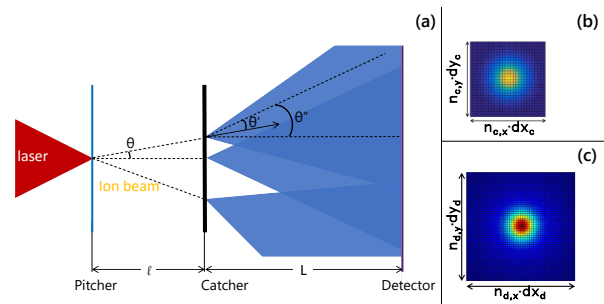


Figure 1: (a) Schematic of the neutron generation process in the pitcher-catcher scheme. An ion beam is generated by the interaction of the laser with the target (pitcher), which then reaches the secondary converter (catcher), leading to the neutron emission. (b) and (c) depict the grids representing the catcher and the detector, respectively.

95 The input for the projectile ion beam in our model
 96 is the angularly-resolved ion spectra. This informa-
 97 tion can either be obtained numerically, by performing
 98 multi-dimensional PIC simulations of the laser-foil in-
 99 teraction, or experimentally, by using for example an-
 100 gularly distributed high-resolution Thomson Parabola
 101 Spectrometers (TPS) [14]. The angularly resolved ion
 102 spectra can be represented by a function $\frac{d^2 N_{ion}}{dE d\Omega}(E, \theta, \varphi)$,
 103 where E is the ion energy, (θ, φ) are the angles defin-
 104 ing the direction of a given beamlet of ion, and Ω stands
 105 for solid angle. For simplicity, one may assume the ion
 106 beam produced by the laser-foil interaction to be cylin-
 107 drically symmetrical about θ .

108 The catcher in the model was designed as a two di-
 109 mensional matrix ($n_{c,x} \times n_{c,y}$ cells), where the grid size
 110 ($dx_c \times dy_c$) can be chosen depending on the desired res-
 111 olution and accuracy, being $dx_c = dy_c = 200 \mu\text{m}$ the
 112 resolution for the simulations here shown. The spec-
 113 trum of ions arriving at each grid point on the catcher
 114 ($dN_{ion,(x,y)}/dE$) is calculated from the input ion spectrum

115 to the code (as mentioned above) for a given pitcher-to-
 116 catcher distance (l). In order to obtain the neutron flux
 117 distribution across a plane parallel to the catcher, the
 118 detector in the code was modelled as a two dimensional
 119 array of $n_{d,x} \times n_{d,y}$ cells of size $dx_d \times dy_d$. This detec-
 120 tor configuration mimics the response of CR39 nuclear
 121 track detectors typically used in neutron generation ex-
 122 periments [6, 15], allowing for a direct comparison
 123 between the simulations and the experimental data.

124 Neutron generation from each grid point of the
 125 catcher was calculated by using the tabulated data for
 126 the angularly-resolved neutron yield, that can either be
 127 found in the literature, or be obtained by running Monte
 128 Carlo simulations [12, 13] for different ion energies. In
 129 this paper we used the tabulated data for $d(d,n)^3\text{He}$ re-
 130 action provided by Davis *et al.* [12], which was one
 131 of the main reactions producing neutron in the experi-
 132 ment reported in [6]. The $d(d,n)^3\text{He}$ reaction is also an
 133 efficient fusion reaction for moderate-energy deuterons,
 134 which is suitable for studying the effect of the input ion
 135 beam spectrum and divergence on the neutron beam di-
 136 vergence. The tabulated neutron yield per incident ion,
 137 given in Ref. [12], along different angles of neutron
 138 emission and for different projectile ion energies were
 139 interpolated to obtain a function $Y_n(E, \theta')$, where θ' is
 140 the neutron emission angle with respect to the incident
 141 ion beam. Using this function, the neutron flux at a
 142 given pixel of the detector ($F_{n,(x_d,y_d)} = N_{n,(x_d,y_d)}/dx_d dy_d$)
 143 is calculated as the sum of the fluxes reaching that pixel,
 144 generated at each point on the catcher. This can be ex-
 145 pressed mathematically as

$$N_{n,(x_d,y_d)} = \sum_{(x_c,y_c)} \sum_E Y_n(E, \theta') \cdot N_{ion,(x_c,y_c)}(E)$$

146 where, $\theta' = \tan^{-1} \left(\sqrt{(x_d - x_c)^2 + (y_d - y_c)^2} / L \right)$ and L is
 147 the catcher-to-detector distance.

148 3. Results

149 In order to study the beamed neutron emission ob-
 150 served in our experiment [6] employing the petawatt
 151 arm of the VULCAN laser at Rutherford Appleton Lab-
 152 oratory (RAL), STFC, UK[16], we used the experimen-
 153 tally measured deuteron spectrum as the input to our
 154 model. The ion beams in the experiment were pro-
 155 duced by irradiating 10 μm -thick deuterated plastic foils
 156 with a p-polarised laser pulse of $\sim 200\text{ J}$ energy and
 157 $\sim 750\text{ fs}$ duration, focussed down to a spot of $\sim 6\ \mu\text{m}$
 158 (FWHM) on the target, reaching a peak intensity in ex-
 159 cess of 10^{20} W cm^{-2} . The ion beam spectrum was di-
 160 agnosed along different emission angles ($-8^\circ, 0^\circ, 21^\circ$

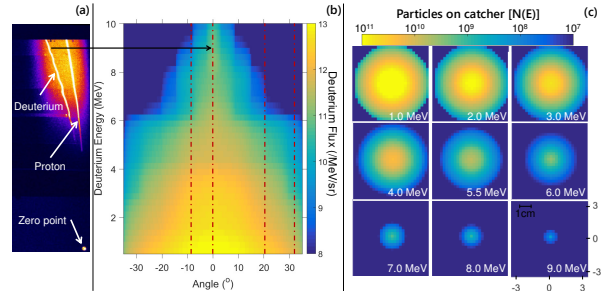


Figure 2: (a) A typical raw data obtained by a TPS diagnosing ion spectrum along the target normal direction. (b) Angularly resolved deuteron spectrum reconstructed from the data obtained by four TPS measurements along different angles (as shown by the dashed line) with respect to the target normal direction. (c) Spatial profiles of deuteron beam for different energies at the catcher plane.

161 and 32°) with respect to the target normal by employing
 162 Thomson Parabola Spectrometers (TPS)[14]. Due to the
 163 limitation of TPS in retrieving the spectrum of overlap-
 164 ping species, a differential filtering technique [17] was
 165 implemented to discriminate the deuterium ions from
 166 the overlapping species with equal charge-to-mass ra-
 167 tio, such as C^{6+} and O^{8+} originated from the target
 168 and hydrocarbon contaminant layers. A typical raw data
 169 obtained along the target normal direction is shown in
 170 Fig. 2(a). A comparison between on-axis proton and
 171 deuteron spectra obtained from the TPS data is shown
 172 in Ref. [6]. The deuteron spectra obtained from the
 173 different TPS were used to reconstruct the full beam
 174 profile, as shown in Fig. 2(b), while assuming an axis-
 175 symmetrical beam profile. The data shows a divergent
 176 ($\sim 30^\circ$ FWHM, $\sim 60^\circ$ full cone) beam of deuterons with
 177 an exponential spectrum, with the highest energies pro-
 178 duced along the target normal direction with a narrow
 179 ($\sim 15^\circ$ full cone) beam divergence, as expected from
 180 the TNSA mechanism for such laser and target param-
 181 eters [18].

182 The angularly-resolved deuteron spectra shown in
 183 Fig. 2(c) was used in our code to simulate the neu-
 184 tron generation in the catcher placed at a distance of
 185 $l = 5\text{ mm}$ from the ion source (which represents the
 186 point of laser interaction with the pitcher target). The
 187 flux distribution of the deuterons of different energies
 188 at the front surface of the catcher are shown in Fig. 2(c),
 189 which was obtained by using the beam profile shown in
 190 Fig. 2(b).

191 Despite of the moderate energies of the ions and the
 192 broad emission angle produced in the experiment, the
 193 simulation shows a directional beam-like emission of
 194 neutrons from the catcher target, as shown in Fig. 3
 195 (showing neutron flux distribution across the detector

196 plane placed at a distance $L = 15$ mm from the catcher),
 197 with a Full Width at Half Maximum (FWHM) diver-
 198 gence of $\sim 62^\circ$ and maximum flux along the ion beam
 199 axis. The simulated neutron beam profile is similar to
 200 that obtained from the experiment (FWHM of $(70 \pm 10)^\circ$)
 201 [6]). Since the simulated neutron beam profile was ob-
 202 tained by considering only the $d(d,n)^3\text{He}$ reaction, the
 203 residual difference between the simulated and experi-
 204 mental neutron beam profile is most likely due to a
 205 range of additional nuclear reactions taking place in the
 206 catcher in the latter case. As discussed in Ref. [6], due
 207 to the higher flux and higher energy protons produced
 208 from the pitcher target (as can be seen in Fig. 2(a)), the
 209 proton-induced deuteron breakup reaction ($d(p,n+p)^1\text{H}$)
 210 contributes significantly towards the total neutron yield.
 211 Due to the reaction kinematics, this nuclear reaction
 212 is expected to produce a narrow neutron beam diver-
 213 gence, similar to that obtained for the $d(d,n)^3\text{He}$ reac-
 214 tion. However, a detailed simulation for the $d(p,n+p)^1\text{H}$
 215 case could not be carried out due to the insufficient re-
 216 action cross-section available in the literature.

In order to study the effect of the projectile ion beam
 parameters on the neutron beam divergence, we car-
 ried out a set of simulations by varying the input spec-
 trum of the ions, as expected to be produced by TNSA
 mechanism at different laser intensities. The ion tem-
 perature and the cut-off ion energy in the TNSA mech-
 anism scale with the temperature of the hot electrons

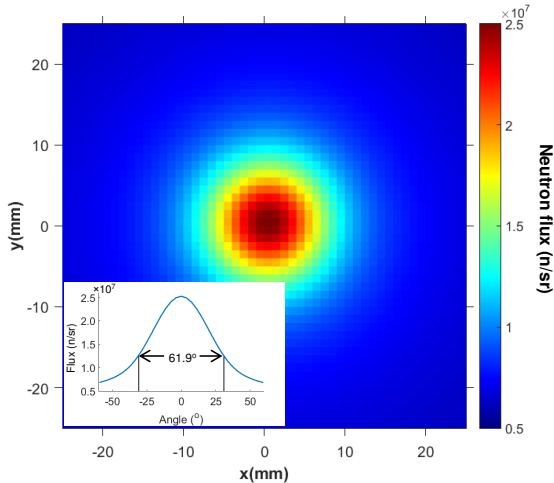


Figure 3: Simulated neutron beam reaching a flat detector in front of the catcher. Inset shows the lineout of the neutron beam profile across the detector, which also represents the emission angle of neutrons with respect to the ion beam axis. The divergence of the neutron beam (FWHM) is $\sim 62^\circ$.

produced by the interaction, which broadly scales as $\sqrt{I_L \lambda^2}$ [9, 19, 20, 21], where I_L and λ stand, respectively, for the intensity and the wavelength of the incident laser. The divergence of the ions produced by the TNSA mechanism also varies within the beam depending on its energy [18] - ions with higher energy are emitted with a lower divergence. Assuming a flat-top flux profile within the ion beam divergence, and the following divergence profile as a function of ion energy (as reported for \sim ps lasers in Ref. [18], which closely matches with the observed divergence shown in Fig. 2(b)),

$$\theta_D(E, E_{max}) = \begin{cases} 62 & E < E_{max}/2 \\ 107.4 - 90.9 \cdot \frac{E}{E_{max}} & E \geq E_{max}/2 \end{cases}, \quad (1)$$

we modelled an input TNSA beam profile for our simulations as a function of laser intensity, as given by

$$\frac{d^2 N_{ion}}{dE d\Omega} = \frac{dN_{ion}}{dE} \Big|_{\substack{E < E_{max} \\ \theta < \theta_D}} \propto \exp\left(-\frac{E}{k_B T(I_L)}\right) \quad (2)$$

A set of simulations were carried out by varying the ion beam temperature $k_B T(I_L)$. The cut-off energy for the deuterons as a function of laser intensities was assumed as $E_{max}(I_L) \propto 10^{-9} \sqrt{I_L}$ MeV, where the proportionality constant was calculated using the maximum deuteron energy obtained in our experiment, shown in Fig. 2(b).

The FWHM divergence of the neutron beam obtained from the simulations is shown in Fig. 4. One can see how the neutron beam divergence reduces significantly with an increase in the ion beam temperature. While a nearly isotropic emission for low ion temperatures is produced, the neutron beam divergence can be reduced below 50° using higher power lasers than that used in our experiment. Intense lasers will produce ions at higher energies, which will provide two-fold enhancement to the on-axis neutron flux - (1) neutron yield per incident ion will increase significantly due to their deeper penetration into the catcher, (2) higher anisotropy due to differential cross-section and kinematics (see Eq. 2 in Ref. [6]). An alternative approach for increasing the flux and energy of ions other than protons, which are preferentially accelerated by the TNSA mechanism, would be to use some special technique to eliminate the hydrogen contamination layer at the rear side of the pitcher target, such as depositing a layer of heavy water contamination for enhancing the deuteron acceleration [22].

The rate of decrease in the neutron beam divergence slows down towards the higher temperatures, as visible in Fig. 4. The nearly constant divergence of $\sim 30^\circ$ obtained for the high ion temperatures is due to the, albeit

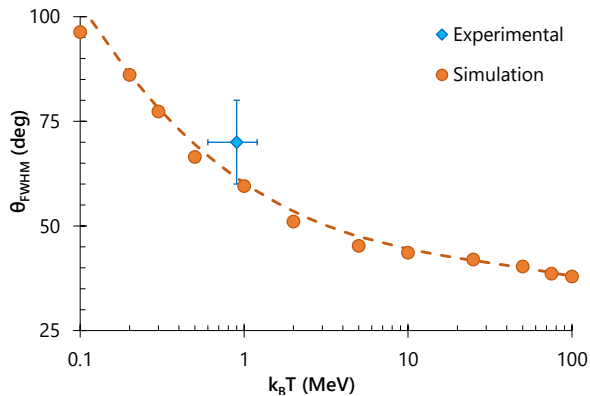


Figure 4: Neutron beam divergence (FWHM) as a function of the ion beam temperature obtained from our simulations. The blue point shows the beam divergence obtained for the $d(d,n)^3\text{He}$ reaction using the deuteron beam profile obtained from our experiment discussed above.

small, intrinsic divergence ($\sim 15^\circ$) of the highest energy ions produced by the TNSA mechanism. This limitation in the neutron beam divergence can be easily eliminated by focussing the ion beams on the catcher, for example by using one of the several schemes reported in literature, such as permanent/pulsed magnetic focusing devices [23, 24, 25], laser-driven micro-lens[26], hemi-spherical targets [27], shaped targets [28] etc. Using a focussed beam of ions with narrow energy band can also help reducing the pulse duration of emitted fast neutrons, as recently reported by Higginson *et al.* [29].

4. Conclusions

We presented results obtained from a numerical model simulating the neutron beam generation by laser-driven ions in a pitcher-catcher scenario. Simulation results are broadly consistent with the neutron beam profile observed in the experiment while using the experimentally measured ion beam profile in the simulation. By varying the ion beam parameters, simulations predict improvement in the neutron beam divergence with an increase in the ion beam temperature and cut-off energy, as expected from the TNSA mechanism at higher laser intensities. Further experimental measurements with improved ion beam parameters would be required to benchmark the simulated trend for neutron beam divergence.

5. Acknowledgements

The authors acknowledge funding from EPSRC [EP/J002550/1-Career Acceleration Fellowship held by S. K., EP/L002221/1, EP/K022415/1, EP/J500094/1. Authors acknowledge support of engineering, target fabrication and experimental science groups of Central Laser Facility of STFC, UK.

- [1] L. Gray, J. Read, Treatment of cancer with fast neutrons, *Nature* 152 (1943) 53.
- [2] A. Buffler, Contraband detection with fast neutrons, *Radiation Physics and Chemistry* 71 (3) (2004) 853–861.
- [3] D. Vartsky, I. Mor, M. Goldberg, D. Bar, G. Feldman, V. Dandendorff, K. Tittelmeier, M. Weierganz, B. Bromberger, A. Brezskin, Novel detectors for fast-neutron resonance radiography, *Nuclear Instruments and Methods in Physics Research Section A: Accelerators, Spectrometers, Detectors and Associated Equipment* 623 (1) (2010) 603–605.
- [4] L. Perkins, B. Logan, M. Rosen, M. Perry, T. D. de la Rubia, N. Ghoniem, T. Ditmire, P. Springer, S. Wilks, The investigation of high intensity laser driven micro neutron sources for fusion materials research at high fluence, *Nuclear Fusion* 40 (1) (2000) 1.
- [5] A. Wiedenmann, U. Keiderling, K. Habicht, M. Russina, R. Gähler, Dynamics of field-induced ordering in magnetic colloids studied by new time-resolved small-angle neutron-scattering techniques, *Physical review letters* 97 (5) (2006) 057202.
- [6] S. Kar, A. Green, H. Ahmed, A. Alejo, A. Robinson, M. Cerchez, R. Clarke, D. Doria, S. Dorkings, J. Fernandez, et al., Beamed neutron emission driven by laser accelerated light ions, *New J. Phys.*, **18**, 053002 (2016).
- [7] A. Alejo, H. Ahmed, A. Green, S.R. Mirfayzi, M. Borghesi, S. Kar, Recent Advances in laser-driven neutron sources, *Il Nuovo Cimento C* (In press)
- [8] S. Atzeni, J. Meyer-ter Vehn, *The Physics of Inertial Fusion: Beam-Plasma Interaction, Hydrodynamics, Hot Dense Matter: Beam-Plasma Interaction, Hydrodynamics, Hot Dense Matter*, Vol. 125, Oxford University Press, 2004.
- [9] A. Macchi, M. Borghesi, M. Passoni, *Reviews of Modern Physics* 85 (2013) 751.
- [10] Extreme light infrastructure(eli) (<http://www.eli-np.ro/>).
- [11] J. Zou, C. Le Blanc, D. Papadopoulos, G. Chériaux, P. Georges, G. Mennerat, F. Druon, L. Lecherbourg, A. Pellegrina, P. Ramirez, et al., Design and current progress of the apollon 10 pw project, *High Power Laser Science and Engineering* 3 (2015) e2.
- [12] J. Davis, G. Petrov, Angular distribution of neutrons from high-intensity laser-target interactions, *Plasma Physics and Controlled Fusion* 50 (6) (2008) 065016.
- [13] D. B. Pelowitz, et al., *Mcnpx users manual version 2.5.0*, Los Alamos National Laboratory 76.
- [14] D. Gwynne, S. Kar, D. Doria, H. Ahmed, M. Cerchez, J. Fernandez, R. Gray, J. Green, F. Hanton, D. MacLellan, P. McKenna, Z. Najmudin, D. Neely, J. Ruiz, A. Schiavi, M. Streeter, M. Swantusch, O. Willi, M. Zepf, M. Borghesi, Modified thomson spectrometer design for high energy, multi-species ion sources, *Review of Scientific Instruments* 85 (3). doi:10.1063/1.4866021.
- [15] G. Petrov, D. Higginson, J. Davis, T. B. Petrova, J. McNaney, C. McGuffey, B. Qiao, F. Beg, Generation of high-energy ($\lesssim 15$ mev) neutrons using short pulse high intensity lasers, *Physics of Plasmas* (1994-present) 19 (9) (2012) 093106.

- 336 [16] C. Danson, P. Brummitt, R. Clarke, J. Collier, B. Fell, A. Frack- 401
337 iewicz, S. Hancock, S. Hawkes, C. Hernandez-Gomez, P. Hol- 402
338 ligan, et al., Vulcan petawatt ultra-high-intensity interaction
339 facility, *Nuclear Fusion* 44 (12) (2004) S239.
- 340 [17] A. Alejo, S. Kar, H. Ahmed, A. Krygier, D. Doria, R. Clarke,
341 J. Fernandez, R. Freeman, J. Fuchs, A. Green, J. Green, D. Jung,
342 A. Kleinschmidt, C. Lewis, J. Morrison, Z. Najmudin, H. Naka-
343 mura, G. Nersisyan, P. Norreys, M. Notley, M. Oliver, M. Roth,
344 J. Ruiz, L. Vassura, M. Zepf, M. Borghesi, Characterisation of
345 deuterium spectra from laser driven multi-species sources by
346 employing differentially filtered image plate detectors in thom-
347 son spectrometers, *Review of Scientific Instruments* 85 (9).
348 doi:10.1063/1.4893780.
- 349 [18] F. Nürnberg, M. Schollmeier, E. Brambrink, A. Blažević,
350 D. Carroll, K. Flippo, D. Gautier, M. Geißel, K. Harres,
351 B. Hegelich, et al., Radiochromic film imaging spectroscopy of
352 laser-accelerated proton beams, *Review of scientific instruments*
353 80 (3) (2009) 033301.
- 354 [19] P. Mora, Plasma expansion into a vacuum, *Phys. Rev. Lett.* 90
355 (2003) 185002. doi:10.1103/PhysRevLett.90.185002.
356 URL [http://link.aps.org/doi/10.1103/
357 PhysRevLett.90.185002](http://link.aps.org/doi/10.1103/PhysRevLett.90.185002)
- 358 [20] J. Fuchs, P. Antici, E. d’Humières, E. Lefebvre, M. Borghesi,
359 E. Brambrink, C. Cecchetti, M. Kaluza, V. Malka, M. Man-
360 clossi, et al., Laser-driven proton scaling laws and new paths
361 towards energy increase, *Nature Physics* 2 (1) (2005) 48–54.
- 362 [21] L. Robson, P. Simpson, R. Clarke, K. Ledingham, F. Lindau,
363 O. Lundh, T. McCanny, P. Mora, D. Neely, C.-G. Wahlström,
364 et al., Scaling of proton acceleration driven by petawatt-laser-
365 plasma interactions, *Nature Physics* 3 (1) (2006) 58–62.
- 366 [22] A. Krygier, J. Morrison, S. Kar, H. Ahmed, A. Alejo, R. Clarke,
367 J. Fuchs, A. Green, D. Jung, A. Kleinschmidt, et al., Selec-
368 tive deuterium ion acceleration using the vulcan petawatt laser,
369 *Physics of Plasmas* (1994-present) 22 (5) (2015) 053102.
- 370 [23] M. Schollmeier, S. Becker, M. Geißel, K. Flippo, A. Blažević,
371 S. Gaillard, D. Gautier, F. Grüner, K. Harres, M. Kimmel, et al.,
372 Controlled transport and focusing of laser-accelerated protons
373 with miniature magnetic devices, *Physical review letters* 101 (5)
374 (2008) 055004.
- 375 [24] M. Nishiuchi, I. Daito, M. Ikegami, H. Daido, M. Mori,
376 S. Orimo, K. Ogura, A. Sagisaka, A. Yogo, A. Pirozhkov,
377 et al., Focusing and spectral enhancement of a repetition-rated,
378 laser-driven, divergent multi-mev proton beam using perma-
379 nent quadrupole magnets, *Applied Physics Letters* 94 (6) (2009)
380 061107.
- 381 [25] S. Ter-Avetisyan, M. Schnürer, R. Polster, P. Nickles, W. Sand-
382 ner, First demonstration of collimation and monochromatisation
383 of a laser accelerated proton burst, *Laser and Particle Beams*
384 26 (04) (2008) 637–642.
- 385 [26] T. Toncian, M. Borghesi, J. Fuchs, E. d’Humières, P. Antici,
386 P. Audebert, E. Brambrink, C. A. Cecchetti, A. Pipahl, L. Ro-
387 magnani, et al., Ultrafast laser-driven microlens to focus and
388 energy-select mega-electron volt protons, *Science* 312 (5772)
389 (2006) 410–413.
- 390 [27] S. Kar, K. Markey, M. Borghesi, D. Carroll, P. McKenna,
391 D. Neely, M. Quinn, M. Zepf, Ballistic focusing of polyener-
392 getic protons driven by petawatt laser pulses, *Physical review
393 letters* 106 (22) (2011) 225003.
- 394 [28] S. Kar, K. Markey, P. Simpson, C. Bellei, J. Green, S. Nagel,
395 S. Kneip, D. Carroll, B. Dromey, L. Willingale, et al., Dynamic
396 control of laser-produced proton beams, *Physical review letters*
397 100 (10) (2008) 105004.
- 398 [29] D. Higginson, L. Vassura, M. Gugiu, P. Antici, M. Borgh-
399 esi, S. Brauckmann, C. Diouf, A. Green, L. Palumbo, H. Pe-
400 trascu, et al., Temporal narrowing of neutrons produced by
high-intensity short-pulse lasers, *Physical review letters* 115 (5)
(2015) 054802.